Indian Journal of Engineering & Materials Sciences
Vol. 32, June 2025, pp. 394-409
DOI: 10.56042/ijems.v32i03.15630

Preparation and characterization of hydroxyapatite reinforced polymeric scaffolds

Duygu Doga Fırat[a], Su Turku Ersoz[a], Fatma BurcuAlp[b*], Ali Emrah Çetin[c] & Muhsin Ciftcioglu[a]

[a]Department of Chemical Engineering, Izmir Institute of Technology, Gulbahce, Urla, Izmir,Turkiye

[b]Department of Chemical Engineering, Suleyman Demirel University, 32260 Çunur, Isparta, Turkiye

[c]Department of Food Engineering, Adana AlparslanTurkes Science and Technology University, Adana, Turkiye

Received: 10 December 2024; accepted: 14 April 2025

Porous HA reinforced PLA/PCL scaffolds with polymer volume percentages in the 7.0–7.6 range have been prepared by solvent-casting/salt leaching technique. The scaffolds have been characterized by conducting gravimetric measurements, FTIR analysis, TGA, X-ray diffraction analysis, compression tests, cell viability tests, and thermal and hydrolytic degradation tests in order to investigate the effect of PLA/PCL, PLA/HA, PCL/HA and PLA/PCL/HA blending on scaffold properties. Porosity of the scaffolds has been determined to be in the 83–92 percent range. The scaffold porosity has decreased with HA content. The water absorption of the scaffolds has been found to be in between 400 and 750%. The yield strength and the elastic modulus of the scaffolds have been determined to be in the 0.001–0.02 and 5.6–10.6 MPa ranges, respectively. The yield strength of the scaffolds has increased by both PCL and HA contents whereas elastic modulus has increased with PCL content but has decreased with HA content. Mechanical test results have indicated that the addition of HA has increased the strength of the scaffolds while decreasing their flexibility. The activation energies for the thermal degradation of the scaffolds have been determined to be in the 130–398 kJ/mol range and have been shown to be a function of PCL, PLA, and HA content. The hydrolytic degradation behavior of the scaffolds in acetate buffer solutions (pH=4.5) during 127 days and XRD analysis have indicated that the hydrolytic degradation occurring in the amorphous part of the surface film has been diffusion-controlled. The diffusion coefficients of the degradation products in the scaffolds have been estimated to be in the $1.21–4.95\times10^{-13}$ m^2/s range. Cell viability test results have indicated that the composition of the composite scaffold structure has played a determining role in the prepared scaffolds.

Keywords: Hydrolytic degradation, Hydroxyapatite, Poly(ε-caprolactone), Poly(L-lactic acid), Scaffold, Thermal degradation

1 Introduction

Tissue engineering and repairing bone and tissue injuries gained increasing attention over the last 20 years. Bone tissue engineering faces significant difficulties in optimizing materials that mimic bone properties like stiffness along with satisfactory biological properties such as biodegradability and biocompatibility. Various properties like the molecular weight, solubility, shape, hydrophilic/hydrophobic nature of the structure, lubricity, surface energy, water absorption and degradation behavior are taken into consideration in the choise of materials to be used in biomedical applications[1].

Design and fabrication of scaffolds are important subjects for tissue engineering and regenerative medicine research. Scaffold plays a vital role in tissue regeneration and repair. 3D scaffolds with high porosities used in tissue engineering are very useful for cell proliferation. The preparation method dictates the mechanical and chemical properties of the scaffolds. A large number of processing techniques have been developed for accomplishing proper materials design. These preparation techniques each have advantages along with disadvantages that strongly affect the scaffold properties. The solvent casting/ particulate leaching method for example provides a superior control over porosity, pore size and crystallinity compared with other techniques but the prepared materials have limited mechanical properties and contains residual solvents and porogen material[2-3]. Porosity, pore size and fiber diameter can be closely controlled by electro spinning method where the pore size decreases with fiber diameter but scaffolds with limited mechanical properties are generally produced[4]. Porosity and pore size can not be independently controlled in melt molding method which also necessitates higher processing temperatures for non amorphous polymers[5]. High processing temperatures and separate leaching steps are not necessary in freeze drying method but the prepared scaffolds have

*Corresponding author (E-mail:burcualp@sdu.edu.tr)

relatively smaller pore sizes along with the necessary longer processing times. Materials with a nontoxic regular and reproducible architecture can be prepared by 3D printing method with enhanced cell attachment and proliferation but significantly longer processing periods are required to fabricate scaffolds[6]. Porous scaffolds (e.g. sponges or foams) have been used in tissue engineering applications. Pore formation and orientation in the foams can be controlled and they are mechanically more stable compared to mesh structures. Solvent casting and particulate leaching technique was developed for enhancing control over porosity and pore diameter compared to other fabrication methods. Polycaprolactone (PCL), polylactic acid (PLA), polyglycolic acid (PGA) and their copolymer (PLGA) are the most commonly used polymers for porous scaffold preparation[7]. PLA is a bioresorbable polymer which is widely used in medical applications especially as bone implants. PLA and PCL are approved by FDA[8] and have been widely used for orthopedics devices such as screws, pins and plates[9-10], along with controlled drug delivery materials[11-12] and bone regeneration scaffolds[13-14]. PCL attracted significant attention due to its excellent biocompatibility and superior mechanical strength and current biomaterials research is concentrated on improving its poor hydrophilicity and slow degradation behaviour[7]. Hydroxyapatite (HA) is a well-known biocompatible ceramic that has physical and chemical similarity with the mineral components of human bones and teeth which is mainly composed of 65–70% bone HA. The incorporation of HA in polymeric material matrices is mainly conducted for improving strength, increasing porosity, altered cell binding abilities, biocompatibility, bioactivity and osteoconduction properties[9]. The presence of HA in the polymer matrix was found to enhance not only osteoinductivity and osteoconductivity but also tailored the desired degradation behaviour and resorption kinetics of the polymer matrix. By-products formed by the dissolution of aliphatic polyesters create an unfavorable acidic environment for cells, while HA or TCP contribute to the elimination of this unfavorable environment by providing basic resorption[15].

PLA and PCL degrade into acidic monomers by hydrolysis of ester bonds. These acidic monomers can be removed by normal metabolic pathways. Hydrolytic degradation of PLA begins in amorphous regions, which leads to an increase in polymer crystallinity. Generally, hydrolytic degradation of PLA can occur by heterogeneous reactions at the surface or by surface erosion. Following chain scission, the carboxylic end groups act as a self catalyzer increasing the hydrolytic degradation rate[16-18].

A review study on the degradability of polymers for implantable biomedical devices reported that the effect of the pH in the 0-14 range on hydrolysis of solid PLA and hydrolysis of PLA solutions in THF (tetrahydrofuran)[19]. The rate of hydrolytic degradation of solid polymers is expected to be lower than that in polymer solutions due to the lower molecular mobility in solid polymeric phases. The degradation of solid polymers differs from the degradation of polymer solution due to the differences in molecular mobilities in the stated two different phases. The slowest degradation rate for polymer solutions was observed at pH 4, whereas the rate of degradation of solid PLA was not affected by pH. The hydrolysis rate of lactic acid accelerates above pH=4 due to its dissociated form since the pKa of lactic acid is 3.84[20].

PLLA/PCL/HA composites were prepared by a dual technique of freeze extraction and porogen leaching with and without HA. Subsequent long-term (78 weeks) hydrolytic degradation study was conducted by using phosphate buffer (pH=7.4) and 0.02% NaN_3 as an antibacterial and antimicrobial agent[9]. The variation of crystal size of the composites with degradation time were investigated by using XRD data. It was observed that the crystal size of PCL increased as the degradation proceeded, whereas the crystal size of PLLA did not change significantly.

The effects of nano-HA fillers in PLA matrix on the fabrication of uniform porous 3D scaffolds by using a solvent-casting/salt-leaching method were investigated in a recent work[21]. It was suggested that the solvent-casting/salt-leaching method is a practical method for preparing highly porous polymeric scaffolds.

The review of literature on 3D composite PLA/PCL/HA scaffold preparation and degradation indicates that a limited level of research have been conducted up to date on these materials. Injured regions in human body is known to create an acidic environment at about pH 4-5[22]. The investigation of the degradation behavior of these scaffolds in acidic environment may contribute significantly to a better understanding of their characteristics and potential applications.

In this study preparation of 3D biodegradable and non toxic HA reinforced PLA/PCL scaffolds were prepared by solvent-casting/salt leaching technique. The scaffolds were characterized by gravimetric measurements, FTIR analysis, TGA, XRD analysis

and compression tests. The effects of component contents (PLA/PCL, PLA/HA, PCL/HA, PLA/PCL/HA) on scaffold structure, mechanical properties, thermal behaviour, hydrolytic degradation in acidic medium (at pH 4.5) and cytotoxicity were investigated. The hydrolytic degradation of the scaffolds in acetate buffer solutions was carried out for 127 days. Cytotoxicity test was conducted by using the MTT (3-(4,5-dimethylthiazol-2-yl)2,5-diphenyl tetrazolium bromide) method.

2 Materials and Methods

2.1 Scaffold preparation

PLA (Nature Works, ingeo biopolymer 2003D with 1.24 specific gravity), PCL (Sigma-Aldrich; number-average molecular weight = 70,000–90,000, density=1.145 g/cc), HA (Sigma-Aldrich, Calcium phosphate tribasic with density=3.18 g/cc), oleic acid (OA) (Riedel) and dichloromethane (DCM; Merck) were used for the preparation of the polymeric scaffolds.

Porous PLA-PCL-HA scaffolds were prepared by using a salt-leaching technique. A polymeric solution was prepared by dissolving 2.5 grams of polymer in 15 cm3 DCM at room temperature while the solution was mixed with a magnetic stirrer. Predetermined amounts of HA (25–50 wt% of PLA along with couple of drops OA for dispersion) were added to the PLA/PCL solutions and stirred for 24h. Milled 25 g of NaCl crystals were added to the PLA/PCL/HA solution. These salt added scaffold precursor mixtures were further placed in an injector using a spatula and packed tightly with the plunger for the formation of about 9 and 12.5 mm diameter cylindrical scaffold samples and allowed to dry overnight in a fume hood. The scaffolds were further removed from syringes and soaked in warm water (30°C) bath in order to remove the porogen salt crystals. Scaffolds were kept in the water bath while refreshing the water media every 2 hours until the conductivity became equal to pure deionized water conductivity. The salt-free porous scaffolds were dried in a vacuum oven for 24 hours to remove the residual water. The PLA/PCL/HA contents of the 12 different scaffolds prepared in this work are given in Table 1.

2.2 Characterization

2.2.1 Density measurement

The density of the prepared scaffolds were measured by using a precision balance with Archimedes kit (Sartorius) and theoretically calculated. This application determines the density of solid substances using the buoyancy method. Samples 8 mm in height and 9 mm in diameter were used for these tests. Dry and wet weights of five almost identical specimens were determined for each coded scaffold sample. The temperature of the water was measured and recorded to find its density at that temperature. Density of the scaffolds were calculated from equation 1:

$$\rho_{exp} = \frac{W_a*(\rho_w - 0.0012)}{0.99983*G} + 0.012 \quad \ldots (1)$$

Where w_a is the dry weight of the sample, ρ_w density of water at measured temperature, G is the buoyancy of water obtained from Archimedes kit. Theoretical density values of the scaffolds were calculated from equation 2.

$$\frac{1}{\rho_{theoretical}} = \sum \frac{x_i}{\rho_i} \quad \ldots (2)$$

Where x_i is the weight fraction of the components in the composites, ρ_i density of the pure components.

2.2.2 Water absorption of scaffolds

Three dry samples from each coded scaffold group were weighed and then placed in a glass bottle filled

Table 1 — Prepared sample compositions and polymer volume percentages determined for the salt added scaffold precursor mixtures.

Sample No	Sample Code	wt %			Polymer Volume Percentages
		PLA	PCL	HA	
1	PLA-native	100	-	-	7.27
2	PLA85-PCL15	85	15	-	7.32
3	PLA80-HA20	80	-	20	7.22
4	PLA75-PCL25	75	25	-	7.35
5	PLA68-PCL12-HA20	68	12	20	7.27
6	PLA67-HA33	67	-	33	7.17
7	PLA60-PCL20-HA20	60	20	20	7.30
8	PLA57-PCL10-HA33	57	10	33	7.22
9	PLA50-PCL17-HA33	50	17	33	7.25
10	PCL-native	-	100	-	7.59
11	PCL80-HA20	-	80	20	7.54
12	PCL67-HA33	-	67	33	7.49

with 50 mL water. These bottles were degassed under vacuum for 2 hours at room temperature. After the scaffolds were kept in water for 2 h, they were removed and their wet weight (M_{wet}) was measured by gently wiping the surface water with a wet paper napkin. These samples were then vacuum dried for 24 hours to determine the mass of the dried samples (M_{dry}). The water absorption was calculated using equation 3;

$$water\ absorption\ \% = \frac{M_{wet} - M_{dry}}{M_{dry}} x100 \qquad \ldots (3)$$

2.2.3 FTIR analysis

Diffuse reflectance infrared Fourier transform (DRIFT) analysis was used to analyze the chemical structure of the functional groups present in the scaffolds by using Fourier Transform Infrared (FTIR-Excalibur Series) spectroscopy. KBr pellet method was used for OA and HA by FTIR (SHIMADZU FTIR-8400S) spectroscopy. These characterizations were conducted in the 4000 to 400 cm−1 wave number range with a resolution of 4 cm−1 at room temperature.

2.2.4 Compression test

Compression tests were conducted on 12.5/25 mm (D/L) cylindrical scaffold samples according to ASTM-D1621 with force capacities up to 5 kN and speeds up to 2.5 mm/min by using TA- XT Plus Texture Analyser. Elastic modulus of the scaffolds were determined by using the stress-strain plots. The reported results are the average values of at least three measurements.

2.2.5 Cell viability

2.2.5.1 Preparation of cell strains

L929 cell line was used for the cytotoxicity test. Dulbecco's modified eagle media (DMEM), Bio Ind.), fetal bovine serum (FBS Bio Ind.), gentamycin sulfate solution (Bio Ind.), Trypsin EDTA Solution (Bio Ind.), trypan blue, 3- (4,5-dimetiltriazol-2-il) -2,5 difeniltetra-zoliumbromid (MTT, Amresco), and dimethyl sulfoxide (DMSO, Amresco) were used in L929 cell culture and MTT test.

L929 cell cultivated in 75ml corning flasks with DMEM solution containing 50 mL FBS solution and 500 µLgentamisin and incubated at 37°C under a humid atmosphere of 5% CO2 for 24 h. Cells from the thirty fifth passage were used in these experiments. After incubation, cells were detached from 75 mL flasks with trypsin – EDTA and centrifuged at 800 rpm for five minutes. The liquid part was removed and the sediment was dissolved with 2 mL DMEM solution. The aliquots of this suspension were counted in a Neubauer hemocytometer. The suspension was adjusted to 1 x 10^4 cells/well and inoculated into 24 wells plate.

2.2.5.2 Cytotoxicity test

Prepared scaffolds were tested for cell viability by MTT method. The L929 cells were seeded into a 24 wells plate for 24 hours at 37°C with 5% CO2 humidified incubator. The scaffolds (8mm height and 9 mm diameter) were sterilized with ethyl alcohol and UV light before their placement into the wells. Inoculation of the L929 cells with the scaffold samples were conducted for 24, 48 and 72 hours at 37°C with 5% CO2 humidified incubator. The MTT solution was prepared with MTT dissolved in PBS solution (5mg/mL) and homogenized by ultrasonic bath for 10-15s. The solution was passed through the membrane for sterilization. After incubation, the DMEM solution and scaffolds were removed from the well plates. 600 µL MTT-DMEM stock solution (2.8 mL / 25.2 mL) was added to each well. As the light is harmful to MTT solution, well plates were wrapped with aluminum foil and left to incubate for another 4 h under the same incubation conditions. After 4 h incubation plates were centrifuged (Hettich 30 RF Centrifuge) at 1800 rpm for 10 minutes. Supernatant was removed and 500 µL DMSO was added to wells. The solution color turning purple is an indicator of living cells. The absorbance of the solution were measured at 540 nm by spectrometer (Thermo Varioskan Flash spectrometer). All experiments were performed dublicate, and the cell viability was expressed relative to the control cells.

2.2.6 Thermal analysis

Thermal behaviour of the scaffolds were characterized by TGA (Schimadzu TG-51). About 10 mg scaffold samples were loaded into an alumina pan and heated from room temperature to 600°C by using a 10°C/min heating rate under flowing nitrogen atmosphere (50mL/min). Decompositon kinetics was investigated by using Brodio model in order to evaluate the degradation activation energies.

2.2.7 Hydrolytic degradation in acidic medium

The degradation study was conducted using acetate buffer solution (pH:4.5) for 127 days. The acetate buffer keeps the pH constant during the degradation time. Scaffold samples 9×4 mm (DxL) in size were used in the experiments. Dry scaffolds were weighed

and then placed in plastic tubes filled with 15 mL acetate buffer solution and incubated at 37°C with shaking at 100 rpm. Scaffold samples were withdrawn and rinsed thoroughly with distilled water and vacuum-dried at the end of each degradation cycle (10, 30, and 127 days). The final weights of the samples and the initial dry scaffold weights were determined and used for calculating mass loss percentages at each degradation cycle (labelled as Mt). The 127 days mass loss percentage was labelled as M∞. The reported results are the average values of two measurements.

2.2.8 XRD analysis

Crystal structure of the sacaffolds was identified by X-ray diffractometer (Philips Xpert-Pro) employing Ni-filtered Cu Kα radiation, at a scanning rate of 6° min^{-1} with 2θ ranging from 5° to 70° to determine crystal structure of the original and degraded samples. Crystal size in the scaffolds was calculated by using Debye Scherrer equation (Eq.4):

$$t = \frac{\kappa\lambda}{B\cos\theta} \quad \ldots (4)$$

Here B is the line broadening at half the maximum intensity, θis the Bragg angle, κ is a dimensionless constant that may range from 0.89 to 1.39 depending on the specific geometry of the scattering objects. It was taken as 0.9 in this study for calculation of crystal size from XRD of scaffolds.

3 Results and Discussion

3.1 Density, porosity and water absorption

The effect of PCL and HA content on the porosity and measured density of the scaffolds are shown in Fig. 1. Porosity of the scaffolds was determined to be in the 83-92% range. HA reduced the porosity while increasing the density of the scaffolds. High porosities at similar levels were previously reported for PLA/HA scaffolds[21]. The increase in the density of the PLA/PCL scaffolds may partially be due to the differences in phase structure and the consolidation behaviour of the polmeric matrix as seen in Fig. 1.a. The introduction of nanosized HA crystals modify the phase evolution during solvent removal. The polymeric matrix crystallinity decreases significantly as will be discussed in the following sections on XRD analysis results. The porosity of the PCL/HA scaffolds decreases sharply with HA addition to the lowest level of 83%. The crystallinity of the pure PCL polymer is known to be higher than PLA but was strongly modified with nanosize HA particle addition.

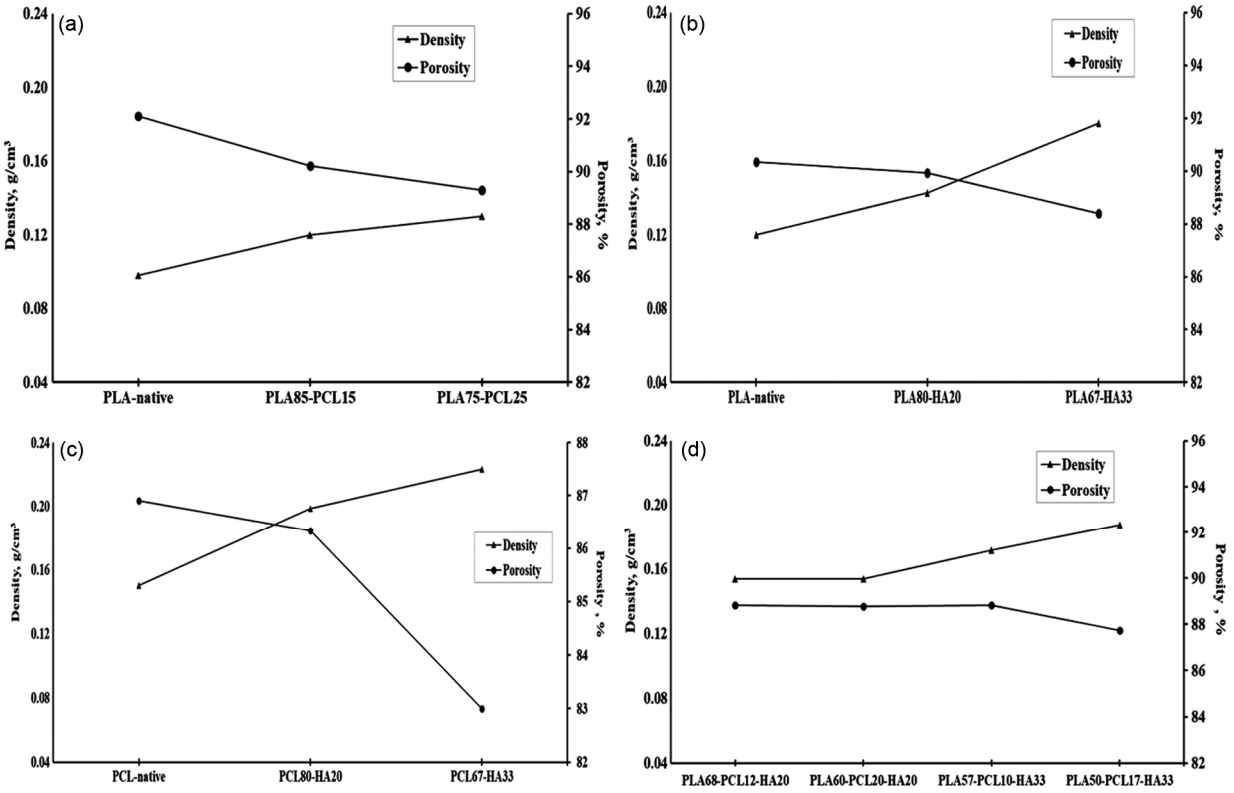

Fig. 1 — Porosity and measured density of the (a) PLA-PCL, (b) PLA-HA, (c) PCL-HA and (d) PLA-PCL-HA scaffolds.

PLA and PCL although are known as hydrophobic polyesters, the pore structure of the scaffolds were filled with water in 2 hours under vacuum. This resulted in significant increases in mass within 2 h as shown in Fig. 2. Fragmentation or no swelling was observed in the scaffolds. It was observed that water absorption was between 400 and 750% since the scaffolds had very high porosities.

Addition of HA reduced the water absorption since those composites had lower porosities. Water absorption results obtained for the scaffolds prepared in this work indicated that almost all the pores were open in nature and the pore structure may be suitable for cell proliferation and growth.

3.2 FTIR analysis

Functional groups present in OA, HA and prepared scaffolds, were investigated by FTIR analysis as shown in Fig. 3(a-e). Wave number assignment of PLA, PCL, OA and HA are given in Table 2. It was previously reported in literature that that characteristic infrared bands of PLA located at 1746 cm^{-1} was due to C=O stretching, 2995 cm^{-1} was due to $–CH_3$ asymmetric stretching, 2946 cm^{-1} was due to–CH_3 symmetric stretching, and 1200 cm^{-1} was due to C–O stretching[23]. The bands at 3278 cm^{-1} and 3221 cm^{-1} were due to OH-COOH functional groups of lactic acid[24]. The C=O stretching was observed at 1774 cm^{-1} in PLA native scaffold in this study as shown in Fig. 3a.

The characteristic infrared bands of PCL at 2949cm^{-1} and 2865 cm^{-1} were due to CH_2 stretching, at 1727 cm^{-1} was due to carbonyl stretching, at 1293 cm^{-1} was due to C–O and C – C stretching in the crystalline phase, at 1240cm^{-1} was due to asymmetric C-O-C stretching, at 1190 cm^{-1} was due to O-C–O stretching, at 1170cm^{-1} was due to symmetric C-O-C stretching, at 1157 cm^{-1} was due to C–O and C–C stretching in the amorphous phase[25-27]. Strong bands were observed such as carbonyl stretching mode at around 1774 cm^{-1} for all the samples. It is revealed that the band at 1296 cm^{-1} was due to the backbone C–C and C–O stretching modes in the crystalline PCL. The characteristic infrared bands of HA located at 963 cm^{-1}, 1095 cm^{-1}, 1036 cm^{-1},were related to PO_4^{-3} ions, at 3570cm^{-1} was due to–OH stretching vibration and at around 1400 cm^{-1} and 870 cm^{-1} were due to CO_3^{-2} ions[28]. The peaks of HA may also

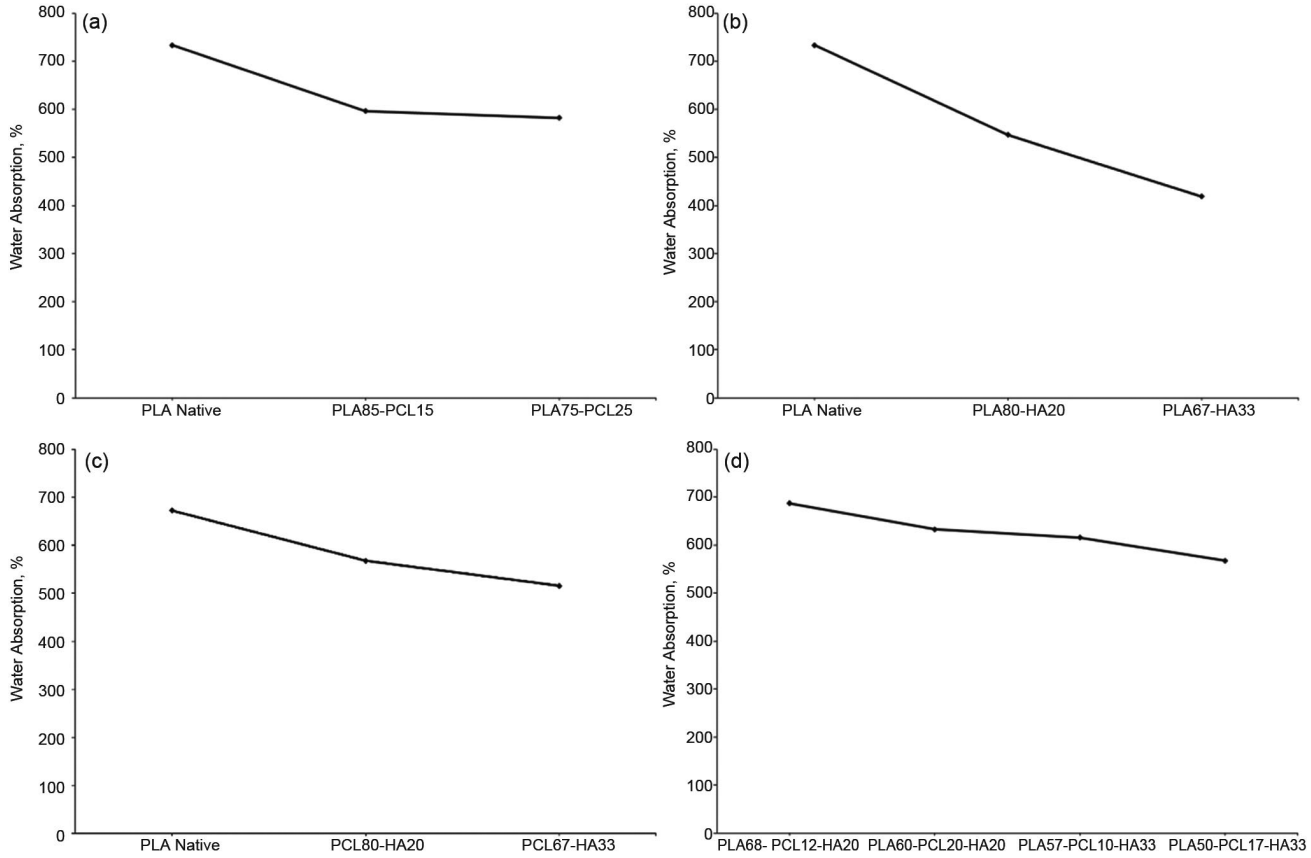

Fig. 2 — Variation in water absorption of the (a) PLA-PCL, (b) PLA-HA, (c) PCL-HA and (d)-PLA-PCL-HA scaffolds.

heavily overlap with the polymer peaks. The presence of HA in the polymeric matrices decreases the absorbance intensity significantly.

3.3 Mechanical test

The compression testing results for the scaffolds are given in Fig. 4. The yield strength of samples are determined from compression test. The yield strength values varied between 0.001 to 0.02 MPa, while the elastic modulus varied between 5.6 to 10.6 MPa. Both PCL and HA addition increased the Yield strength of the PLA based scaffolds (Fig. 4 [a,b,d]). Elastic modulus increased with PCL content and decreased with HA content. HA addition to PCL decreased both Yield strength and elastic modulus (Fig. 4c). Mechanical test results have shown that the addition

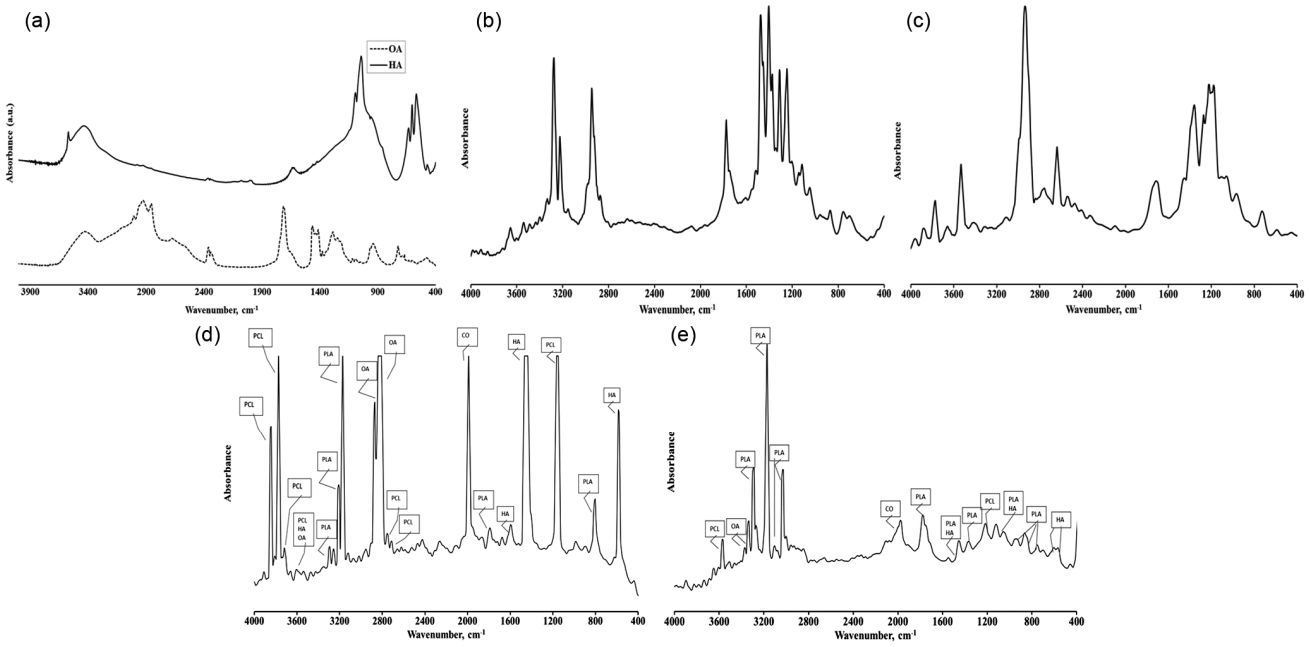

Fig. 3 — FTIR spectra of the (a) Oleic acid and Hyroxyapatite, (b) PLA, (c) PCL, (d) PLA68-PCL12-HA20 and (e) PLA57-PCL10-HA33 scaffolds.

Table 2 — Wave number assignment of PLA, PCL, OA and HA.

PLA		PCL		OA		HA	
Wave number cm^{-1}	Assign.	Wave number cm^{-1}	Assign.	Wave number cm^{-1}	Assign.	Wave number cm^{-1}	Assign.
3279	νOH	3780	νOH	3432	νOH	3559	νOH
3221	νOH	3533	νOH			3429	νOH
2943	CH	2931	$\nu_s CH_2$	2921	$\nu_s CH_2$		
			$\nu_s CH_2$	2861	$\nu_s CH_2$		
		2638	νOH	2669	νOH		
1774	νC=O						
		1712	νC=O	1712	νC=O		
			νC=C			1650	νCO_3
						1637	νCO_3
1477	δCH_3	1450	δCH_2	1471	δCH_2	1454	νCO_3
1408		1365	νCOO	1412	ν_s COO	1417	νCO_3
1307	CH+COC	1249	νCOC	1286	δCH_2		
1246	CH+COC	1219		1247			
1110	νCH_3	1172	νCOC			1106	νPO_4
						1034	νPO_4
1037	$\nu C\text{-}CH_3$	1056	νC-C	1088	νC-C	603	νPO_4
867		956		621		566	νPO_4
740		717		481		471	νPO_4
686	νC=O						

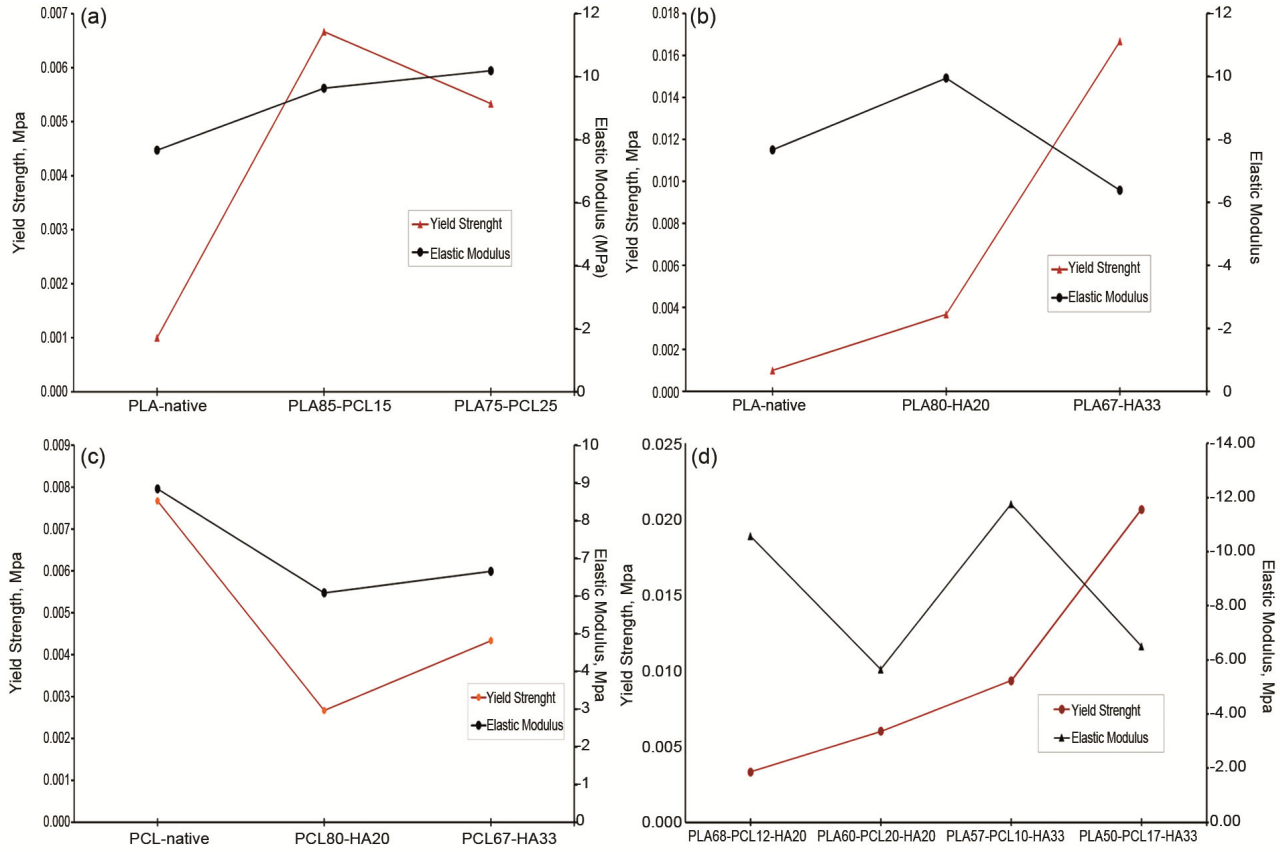

Fig. 4 — Variation of Yield strength and elastic modulus for the (a) PLA-PCL, (b) PLA-HA, (c) PCL-HA and (d) PLA-PCL-HA scaffolds.

of HA increases the strength of the scaffolds while decreasing their flexibility.

3.4 Thermal analysis

Thermograms of prepared scaffolds are shown in Fig. 5. Thermograms present a one-step decomposition process except for PCL native. Degradation peak point of scaffolds were determined from the derivative of thermograms and are given in Table 3. All scaffolds were thermally stable up to 380°C. The additon of PCL and HA to PLA (Fig. 5[a,b,d]) decreased the degradation peak point and increased the amount of ash at 600°C. The addition of HA to PCL did not significantly affect the degradation peak point but increased the amount of ash at 600°C as seen in Fig. 5c.

3.4.1 Thermal degradation kinetics

The decomposition kinetics of the scaffolds was investigated by using the TGA curves and Broido model[29]. The Broido model is based on correlating the rate of mass loss at a constant temperature with fractional decomposition. The Broido's equation is expressed in Equation 5.

$$\ln\left(ln(1/\alpha)\right) = -\frac{E}{RT} + ln\frac{(RZT_m^2)}{\beta E} \quad \ldots (5)$$

where α is the fractional decomposition at any time, $E$is activation energy, Z is a constant, R is the universal gas constant, β is the heating rate, T_m is the temperature of maximum reaction and T is the reaction temperature. E is obtained from slope of the Broido plot. In fact, the apparent activation energy related with the overall mass loss behavior is determined instead of chemical mechanisms involved the thermal degradation process[30].

During the decomposition process, the slope of the Broido plot of ln (ln1/α) vs. 1/T is a straight line (R squared values are 0.99 except forPCL80-HA20 as given in Table 3) as seen in Fig. 6 from which the energy of activation, E_a, was calculated. The E_a, slopes and intercept of Broido plots are given in Table 3. Degradation activation energies of the scaffolds varied between 130-398 kJ/mol. The values of E_a appear consistent with the relative thermal stabilities of the scaffolds. Degradation peak point decreases as the activation energy decreases. The Broido model assumes that thermal degradation occurs in one step.

The thermal degradation mechanism of the PLA/PCL / HA composite is complex because the decomposition of a polymeric material does not occur in single step.

It has been reported that PLA's degradation mechanism involves transesterification reactions. Thermal degradation behavior of PLA and L-lactic acid oligomer composed of HA nanoparticles grafted on the surface of PLA were examined and compared using TGA analysis. The grafted HA particles have a barrier effect decreasing the degradation rate of the HA grafted PLA composite compared to the pure PLA[31]. Similar behavior was observed for the PLA-HA scaffolds investigated in this work. The HA addition to the solvent casted composite scaffolds PCL/HA and PLA/PCL/HA prepared in this work decreased the degradation rates and slightly increased the degradation

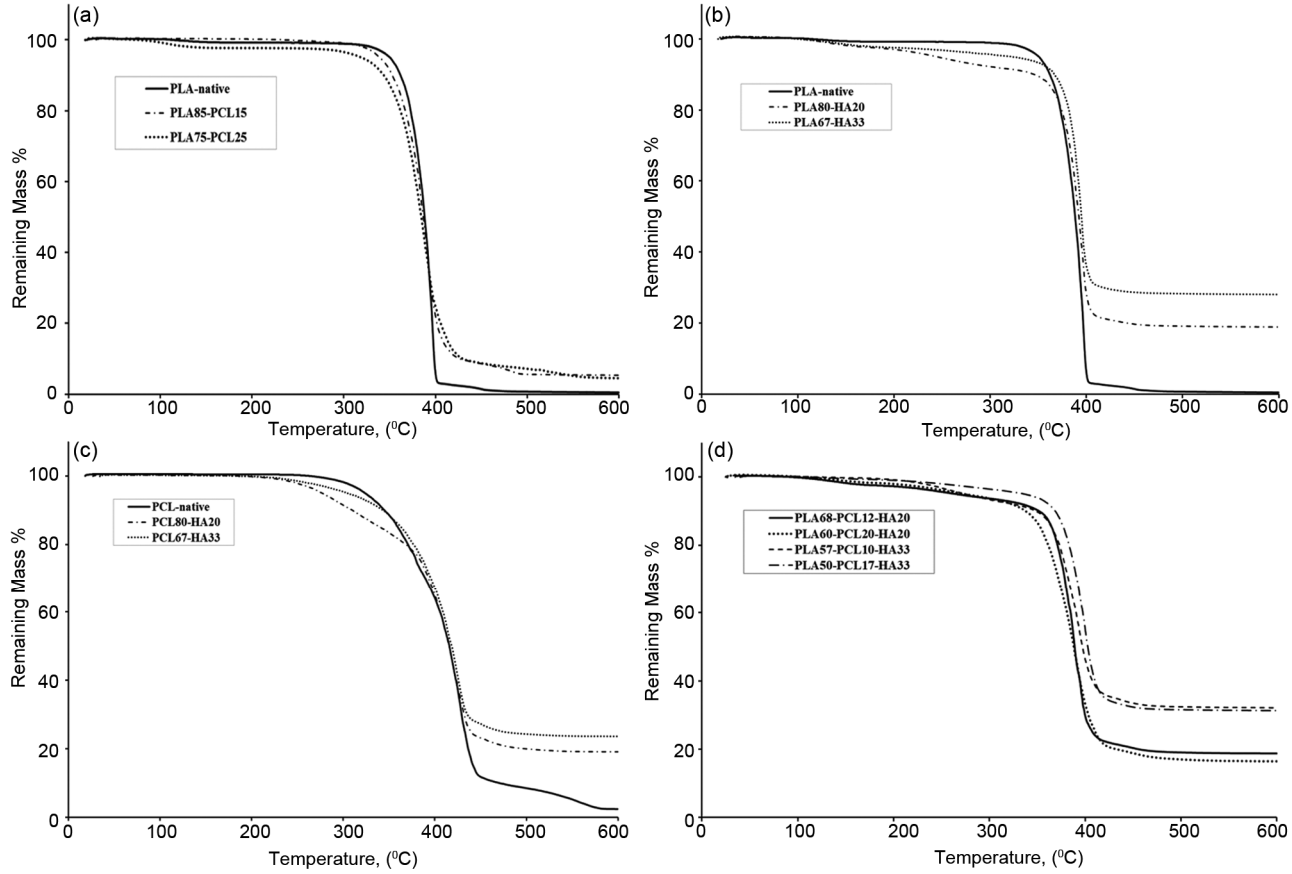

Fig. 5 — TGA thermograms of the (a) PLA-PCL, (b) PLA-HA, (c) PCL-HA and (d) PLA-PCL-HA scaffolds.

Table 3 — Scaffold's degradation peak point, amount of ash at 600°C and degradation activation energy E_a, slope, intercept and R squared value of broido plots.

Sample Code	Degradation Peak Point	Amount of ash at 600°C	E_a(kJ/mol)	Slope	Intercept	R^2
PLA-native	392.6	2.82	273.04	-29850	49.31	0.99
PLA85-PCL15	388.6	5.31	234.19	-24864	42.44	0.99
PLA80-HA20	392.8	18.91	290	-34881	52.439	0.99
PLA75-PCL25	387.5	4.53	189.83	-20143	34.42	0.99
PLA68-PCL12-HA20	391.7	18.74	253.17	-28213	45.61	0.99
PLA67-HA33	392.2	28.01	320.09	-9390.6	57.68	0.99
PLA60-PCL20-HA20	389.3	16.45	187.53	-18457	30.45	0.99
PLA57-PCL10-HA33	392.9	32.12	169.22	-18333	36.77	0.99
PLA50-PCL17-HA33	392	31.28	267.44	-28897	44.02	0.99
PCL-native	425.8	2.31	163.3	-19641	42.81	0.99
PCL80-HA20	425	19.07	78.07	-5061.8	22.89	0.98
PCL67-HA33	423.3	23.67	42.08	-9390.6	23.09	0.99

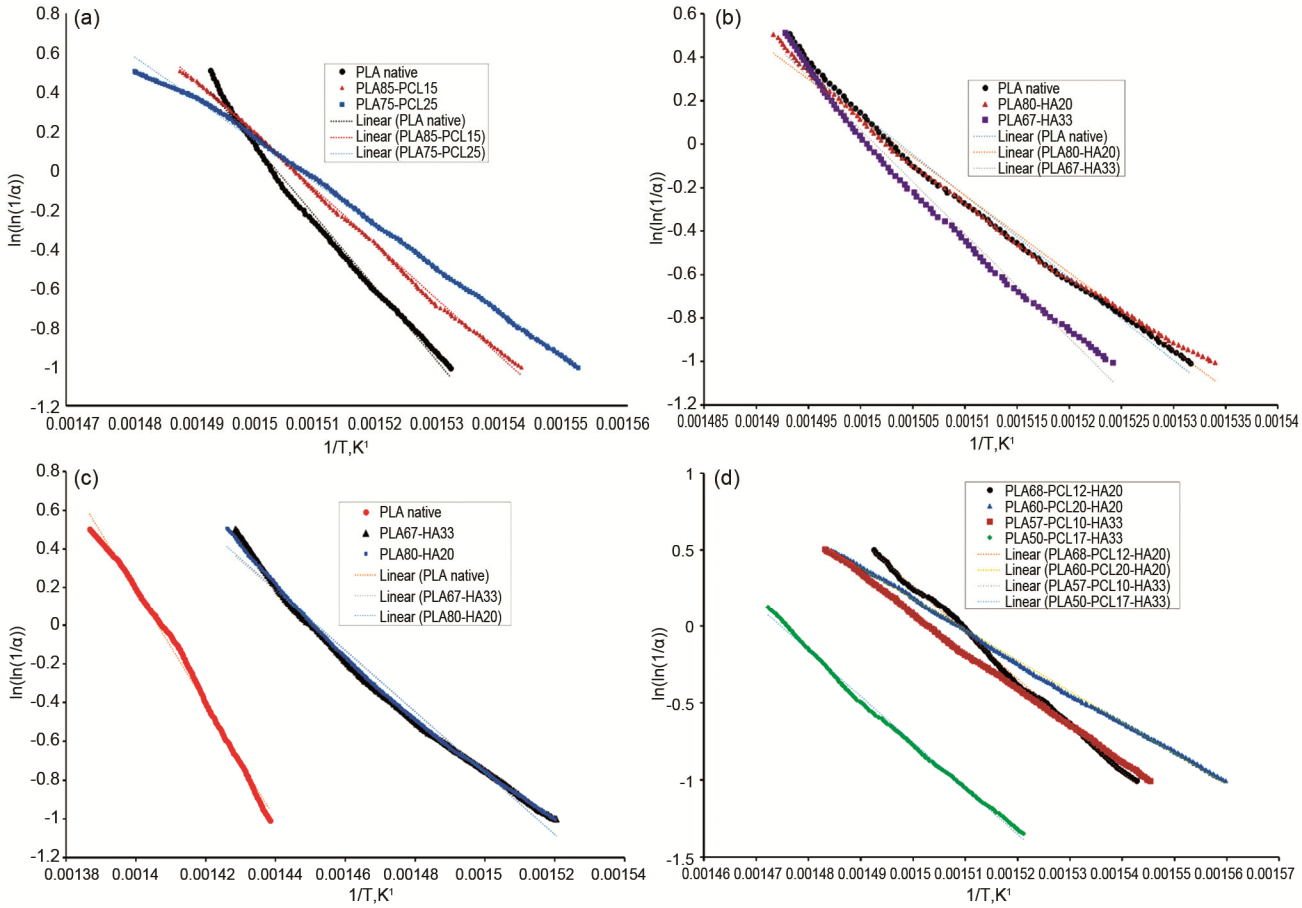

Fig. 6 — Broido plot for the (a) PLA-PCL, (b) PLA-HA, (c) PCL-HA and (d) PLA-PCL-HA scaffolds.

peak point. These variations in the degradation behavior of the scaffolds may also be significantly be affected by the phase structure/consolidation behaviour of the polymeric composites during solvent removal/ processing.

PCL addition to the PLA matrix decreased the activation energy significantly as shown in Fig. 7a. 20 wt% HA addition to the PLA decreased the activation energy whereas 33wt% increased (Fig. 7b) the activation energy. HA addition to PCL decreased the activation energy (Fig. 7c). Amount of PLA decreased, activation energy of PLA/PCL/HA scaffolds decreased as shown in Fig. 7d. The thermal stabilities of the polymer-polymer (PLA/PCL) and polymer-inorganic (PLA-HA; PCL-HA; PLA-PCL-HA) scaffolds were considerably different when compared with the native polymer scaffolds which shows significant interactions between the scaffold components.

3.5 *In Vitro* hydrolytic degradation

The in vitro hydrolytic degradation of scaffolds using acetic acid buffer solution (pH=4.5) at 37°C was carried on for 127 days period. The weight loss and evolution of the crystal size were determined by weight measurements and XRD phase structure analysis.

Fig. 8 illustrates XRD patterns of scaffolds before and after in vitro degradation in acidic medium for 127 days. Sharp peaks were observed in the XRD patterns of samples after degradation. Typical peaks were observed for the PLA phase appear at 2θ value of 16.60°, for the PCL phase appear at 2θ value of 21.80° was the (111) lattice plane and 2θvalue of 24.04° was the (100) lattice plane[9]. The major peaks of HA were observed between 2θ value of 31.80°-32.90° according to reflection on the planes of Miller indices[7,32]. Crystal sizes of the polymeric phases and HA present in the scaffolds were calculated by using Debye-Scherrer equation and are given in Table 4 and Fig. 9. Crystallite size of the HA in the scaffolds before degradation was determined to be in the 4.5-23 nm range.

It is known that the crystallization of the nanocomposites are dramatically increased at very low

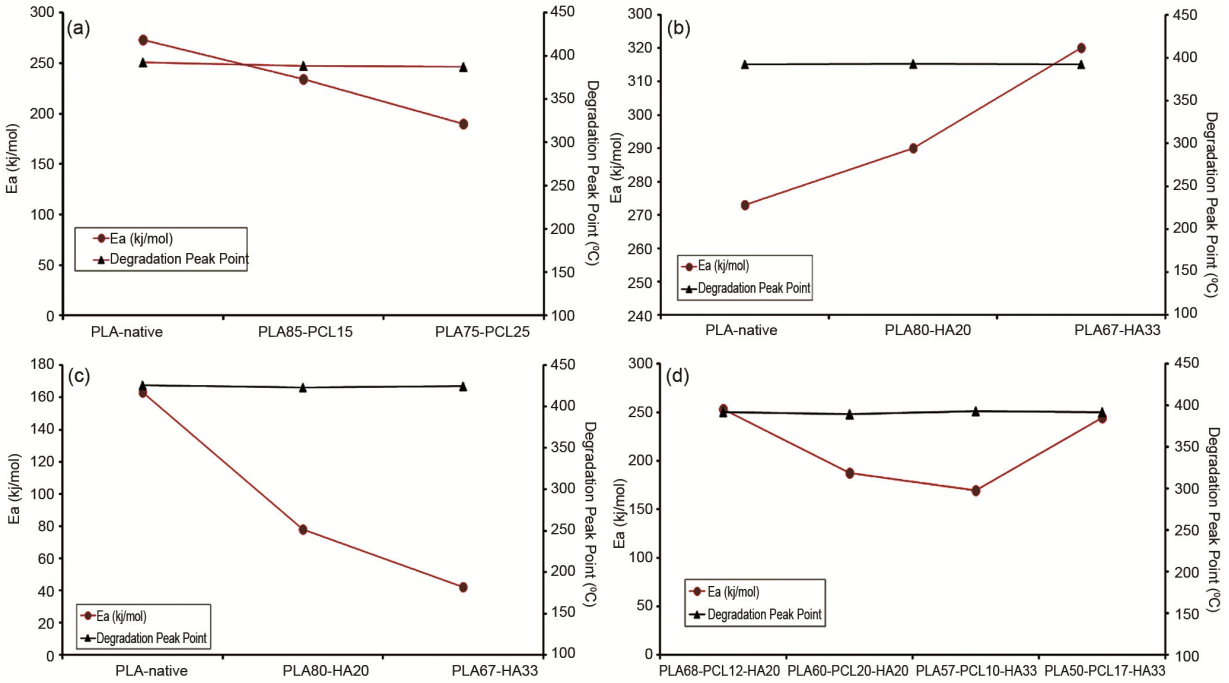

Fig. 7 — Variation of the activation energy and degradation peak point of the (a) PLA-PCL, (b) PLA-HA, (c) PCL-HA and (d) PLA-PCL-HA scaffolds.

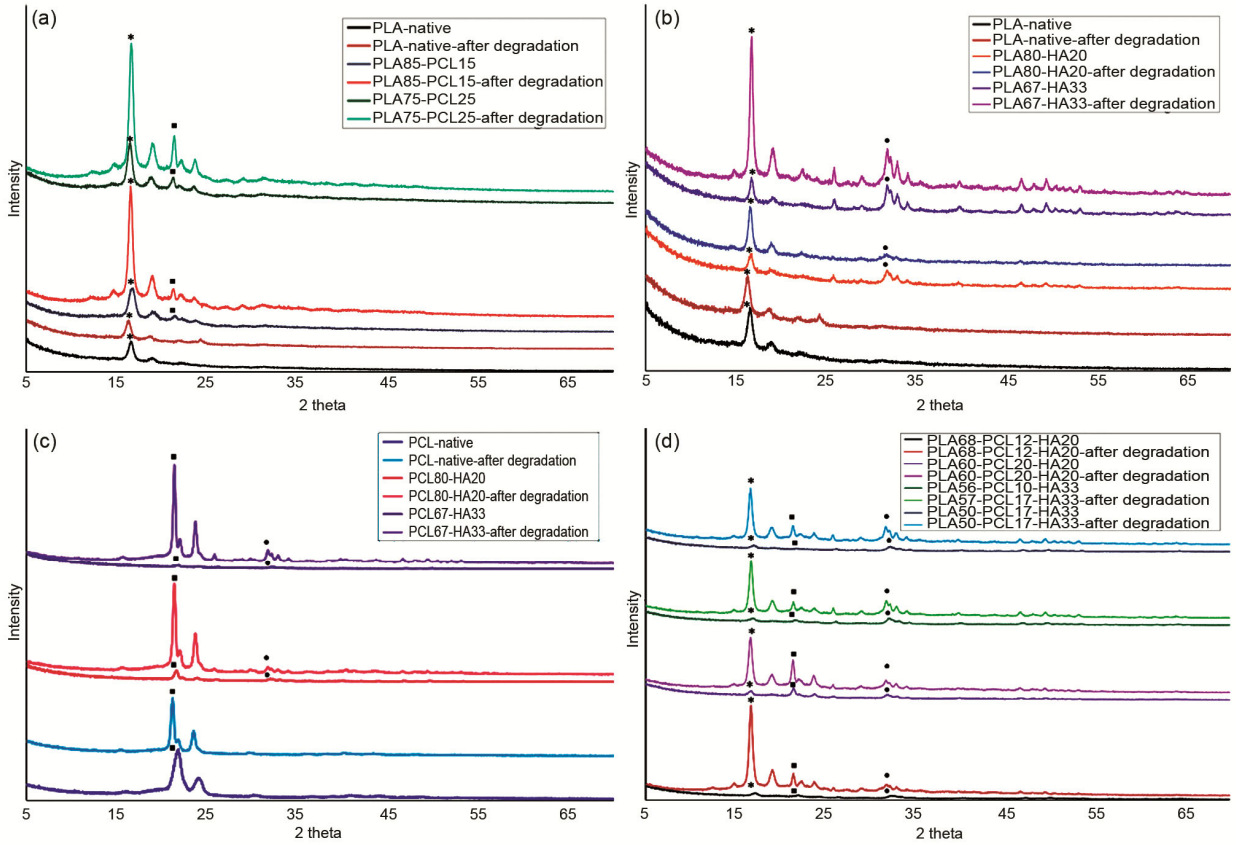

Fig. 8 — XRD pattern of (a) PLA-PCL, (b)PLA-HA, (c) PCL-HA and (d) PLA-PCL-HA scaffolds before and after degradation *in vitro* acidic medium for 127 days (*PLA, ▪PCL, ˙HA).

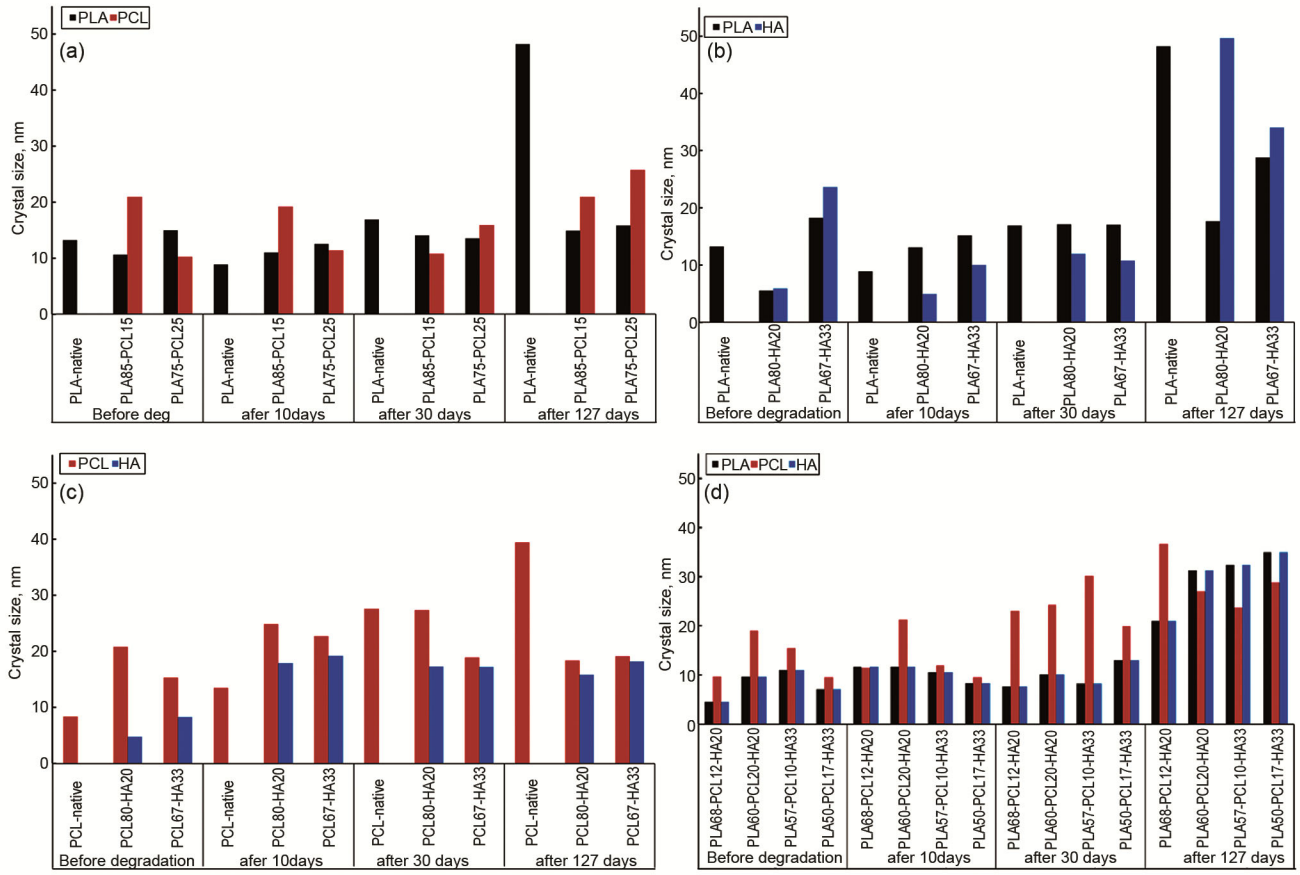

Fig. 9 — Crystal size evolution with degradation time for (a) PLA-PCL, (b) PLA-HA, (c) PCL-HA and (d)-PLA-PCL-HA scaffolds before and after degradation in vitro acidic medium for 127 days.

Table 4 — Calculated crystal sizes of the scaffolds during hydrolytic degradation

Sample Code	Before degradation			After 10 days			After 30 days			After 127 days		
	PLA	PCL	HA	PLA	PCL	HA	PLA	PCL	HA	PLA	PCL	HA
PLA-native	13.24			8.87			16.91			48.25		
PLA85-PCL15	10.65	20.99		11.05	19.23		14.10	10.78		14.92	20.99	
PLA80-HA20	5.51		5.95	13.06		4.93	17.13		11.93	17.67		49.65
PLA75-PCL25	15.04	10.26		12.55	11.43		13.56	15.90		15.88	25.78	
PLA68-PCL12-HA20	4.57	9.69	4.57	11.71	11.43	11.71	7.74	23.08	7.74	20.92	36.72	20.92
PLA67-HA33	18.23		23.63	15.16		10.01	17.08		10.79	28.75		34.02
PLA60-PCL20-HA20	9.70	18.98	9.70	11.64	21.18	11.64	10.17	24.24	10.17	31.24	26.97	31.24
PLA57-PCL10-HA33	10.96	15.46	10.96	10.58	11.99	10.58	8.22	30.13	8.22	32.44	23.65	32.44
PLA50-PCL17-HA33	7.09	9.59	7.09	8.36	9.59	8.36	12.92	19.91	12.92	34.96	28.80	34.96
PCL-native		8.32			13.51			27.57			39.37	
PCL80-HA20		20.77	4.79		24.81	17.92		27.36	17.27		18.36	15.80
PCL67-HA33		15.29	8.31		22.70	19.20		18.89	17.22		19.10	18.20

levels of inorganic additives, such as clay, hydroxyapatite, and starch, but at higher filler contents, the diffusion of polymer chains to the growing crystallites is blocked, and the overall crystallinity reduced with respect to pure material[27]. In this study high HA contents were used and the crystallinity of both PLA and PCL was decreased with HA addition as seen in Fig. 8(b-c). Crystal sizes of polymeric scaffolds were significantly increased after degradation. XRD analysis indicated that hydrolytic degradation occurring from surface of the amorphous part of the scaffolds into the acetate buffer solution was diffusion controlled.

The percentage weight loss behaviour of the scaffolds with degradation time are shown in Fig. 10. The pure polymers PLA, PCL and their composites all had relatively low degradation levels (≤ 5 % mass losses in 127 days) as clearly seen in Fig. 10. The presence of HA in the scaffolds significantly affected the hydrolytic degradation of the scaffolds. The polymer chains were broken during polymer crystallization from the solution in the presence of HA nano particles. The presence of the polymer with smaller chain sizes also accelerated the hydrolytic degradation.

3.6 Hydrolytic Degradation Kinetics

The XRD analysis results have shown that the hydrolytic degradation of the scaffolds was diffusion controlled. The experimental data was analysed by the application of Fick's second law[33]. Diffusion of the polymer into the solution can be represented by Fick's first law Equation 6;

$$J = -D\frac{\partial C_i}{\partial x} \quad \ldots (6)$$

Fick's first law presents a steady state diffusional release. Fick's second law as given in Equation 7 is used for the description of transient phenomena where the concentration profile is not constant during diffusion in one dimension when D is constant.

$$\frac{\partial C}{\partial t} = D\frac{\partial^2 C}{\partial x^2} \quad \ldots (7)$$

General solutions of the diffusion equation can be obtained for certain initial and boundary conditions by assuming the diffusion coefficient constant. Such a solution may consist of a set of error functions or related integrals. Consantration as a function of time given in equation 8 is obtained by differentiating Equation 7.

$$C = \frac{A}{t^{1/2}}\exp\left(-x^2/4Dt\right) \quad \ldots (8)$$

Where A is an arbitrary constant. The above is symmetrical with respect to $x = 0$. As x approaches to infinity consantration approaches to zero. The total amount of substance M diffusing in a cylinder of infinite length and unit cross-section is given by Equation 9,

$$M = \int_{-\infty}^{\infty} C dx \quad \ldots (9)$$

Substituting Eq.8 in Eq.9for C and integrating it Equation 10 is obtained. This solution which describes the spreading by diffusion of an amount of substance M deposited at time t=0 in the plane $x = 0$.

$$\frac{M_t}{M_\infty} = \frac{4}{L}\sqrt{D\frac{t}{\pi}} \quad \ldots (10)$$

Where M_t is the mass loss percent of the scaffolds at time t and M_∞ is the mass loss percent of the scaffolds at infinity, L is the half thickness of the scaffolds, t is the degradation time and D is the diffusivity coefficient. The diffusivity coefficients were

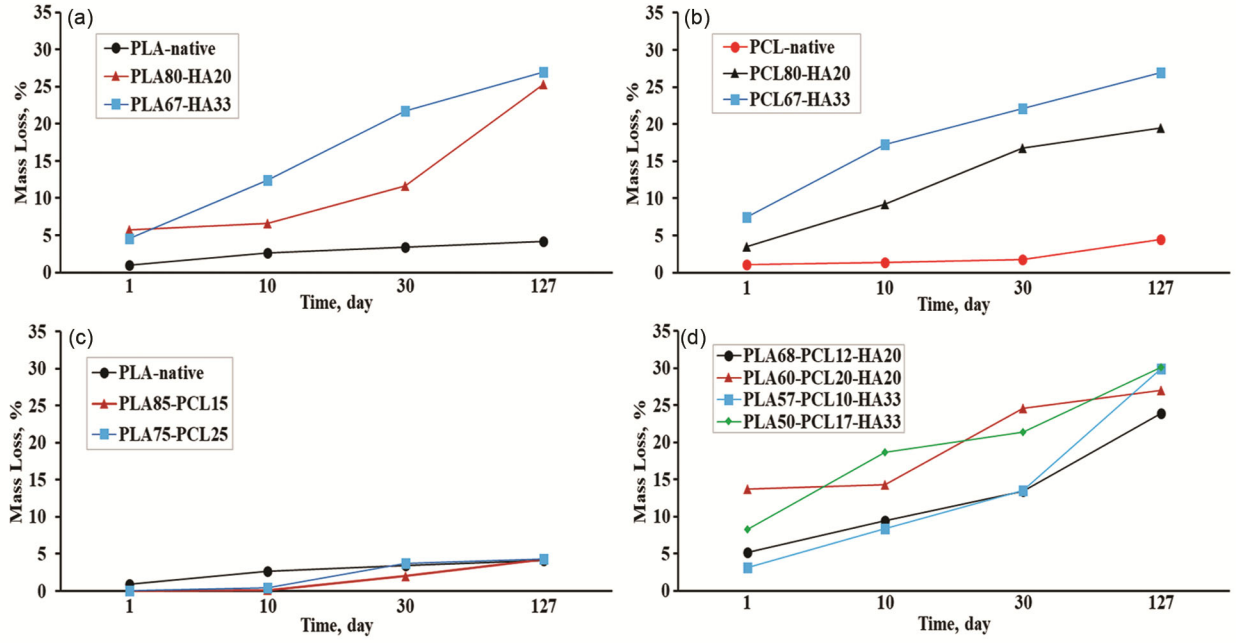

Fig. 10 — The percentage mass loss evolution with degradation time for (a) PLA-PCL, (b) PLA-HA, (c) PCL-HA and (d) PLA-PCL-HA scaffolds before and after degradation in vitro acidic medium for 127 days.

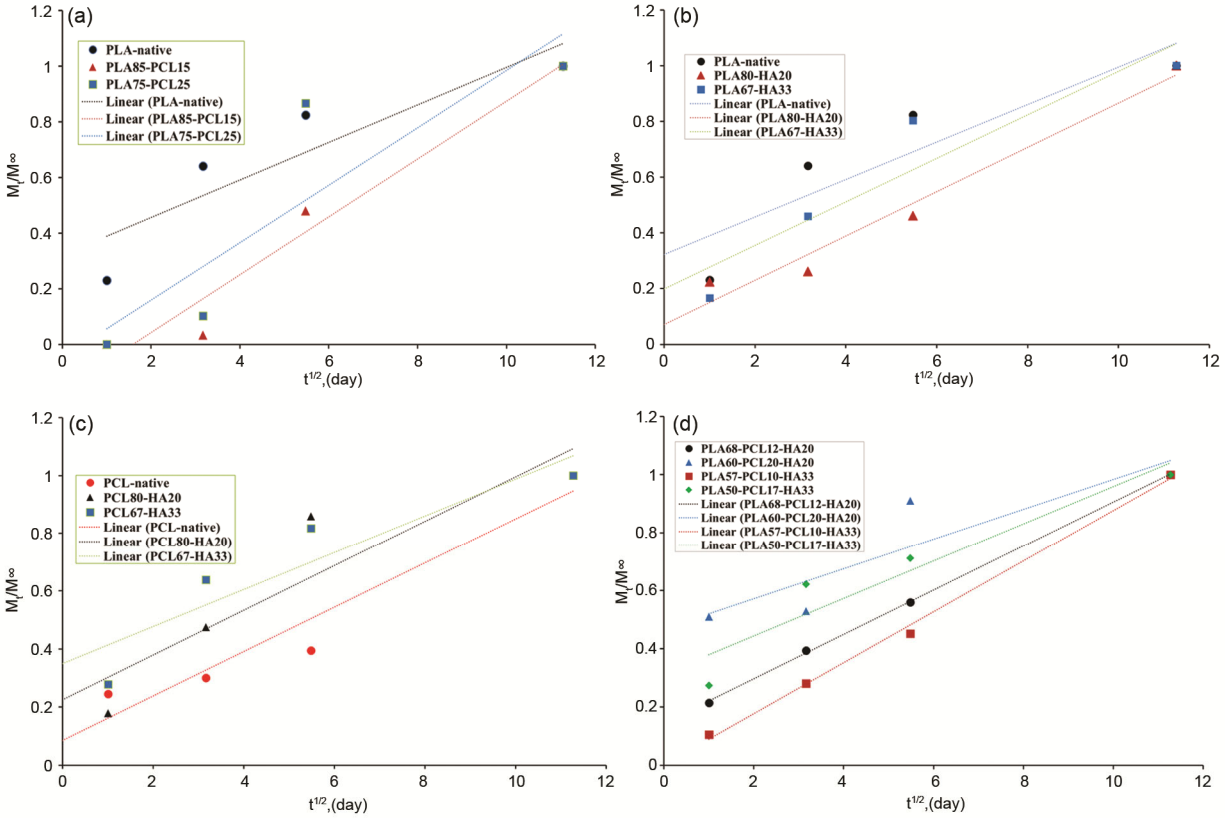

Fig. 11 — The variation of M_t/M_∞ with the square root of the time of degraded in vitro acidic medium for 127 days (a) PLA-PCL, (b) PLA-HA, (c) PCL-HA and (d) PLA-PCL-HA scaffolds.

calculated from slope of M_t/M_∞ versus square root of time plots as shown in Fig. 11. Diffusion coefficient 127 days degraded scaffolds in acidic medium are given in Table 5 along with the slopes and R squared values of M_t/M_∞ versus square root of time plots. Diffusion coefficients of scaffolds were determined to be in between 1.21×10^{-13} and 4.95×10^{-13} m^2/s as can be seen in Fig. 12. Addition of PCL and HA into PLA increased the degradation diffusion coefficients (Fig. 12[a-b]). HA addition to PCL decreased the degradation diffusion coefficient as seen in Fig. 12c. The degradation diffusion coefficients of the PLA/PCL/HA scaffolds varried in the $1.21\text{-}3.51 \times 10^{-13}$ m^2/s range as seen in Fig. 12d which indicates structural dependency of the diffusion phenomena.

Table 5 — Calculated diffusion coefficient value of degraded in vitro acidic medium for 127 days scaffolds, slope and R squared values of M_t/M_∞ versus square root of time plots.

Sample Code	Diffusivity Coefficient x10^{13} [m^2/s]	Slope	R^2
PLA-native	2.08	0.0673	0.81
PLA85-PCL15	4.95	0.1038	0.95
PLA80-HA20	2.90	0.0795	0.96
PLA75-PCL25	4.87	0.103	0.78
PLA68-PCL12-HA20	2.65	0.076	0.99
PLA67-HA33	2.80	0.0781	0.87
PLA60-PCL20-HA20	1.21	0.0515	0.80
PLA57-PCL10-HA33	3.51	0.0874	0.99
PLA50-PCL17-HA33	1.90	0.0643	0.90
PCL-native	2.68	0.0764	0.93
PCL80-HA20	2.72	0.0764	0.83
PCL67-HA33	1.87	0.0639	0.84

3.7 MTT Test

After L-929 cell culturing for 24, 48 and 72 hour periods the viability and proliferation of fibroblast cells were determined by MTT test. MTT results indicated that most of the scaffolds had no toxic effects on fibroblast cells with viability values over 70%[34]as shown in Fig. 13. The PLA content of the scaffolds had a determining effect on long term cell viabilities. The pure PLA scaffold (PLA-native) had a cell viability of 65.7% after 3 days of incubation (Fig. 13 [a-b]). The 2 and 3 day incubated PLA68-PCL12-HA20 composite scaffold had cell viabilities lower than 70% (64.5 and 65.5%, respectively) as seen in Fig. 13d. In contrast to PLA, the addition of PCL increased the cell viability (Fig. 13a). Cell viability

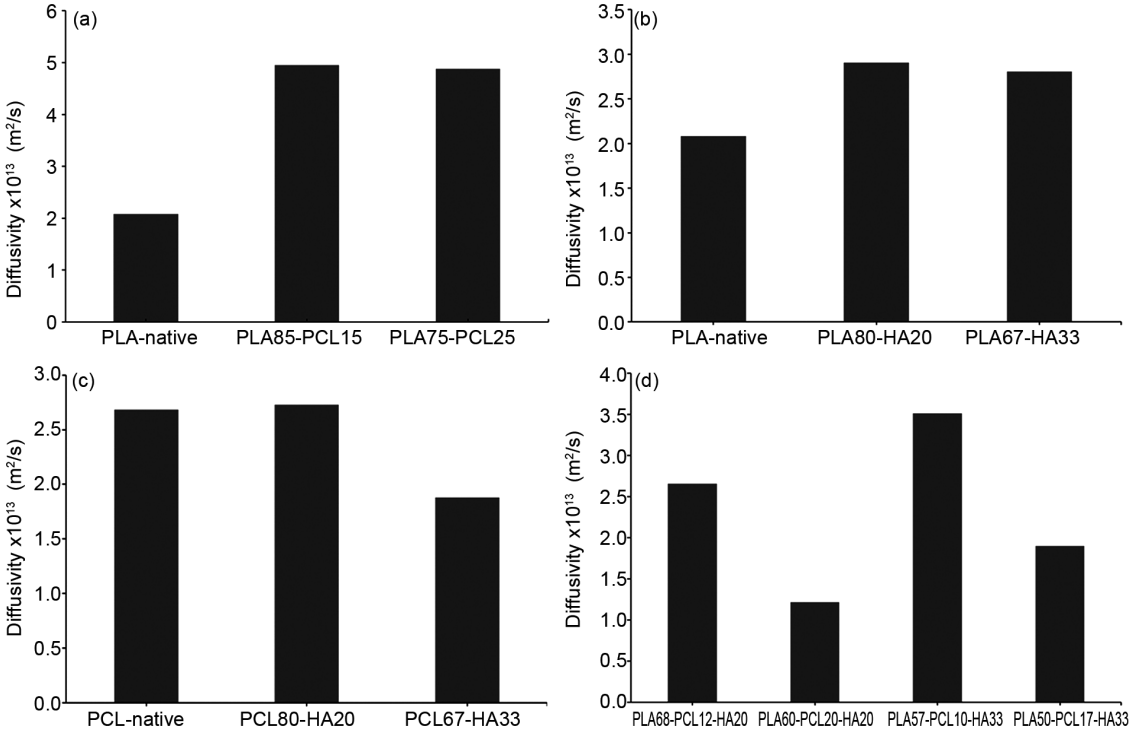

Fig. 12 — The variation of diffusivity coefficient of degraded in vitro acidic medium for 127 days (a) PLA-PCL, (b) PLA-HA, (c) PCL-HA and (d) PLA-PCL-HA scaffolds.

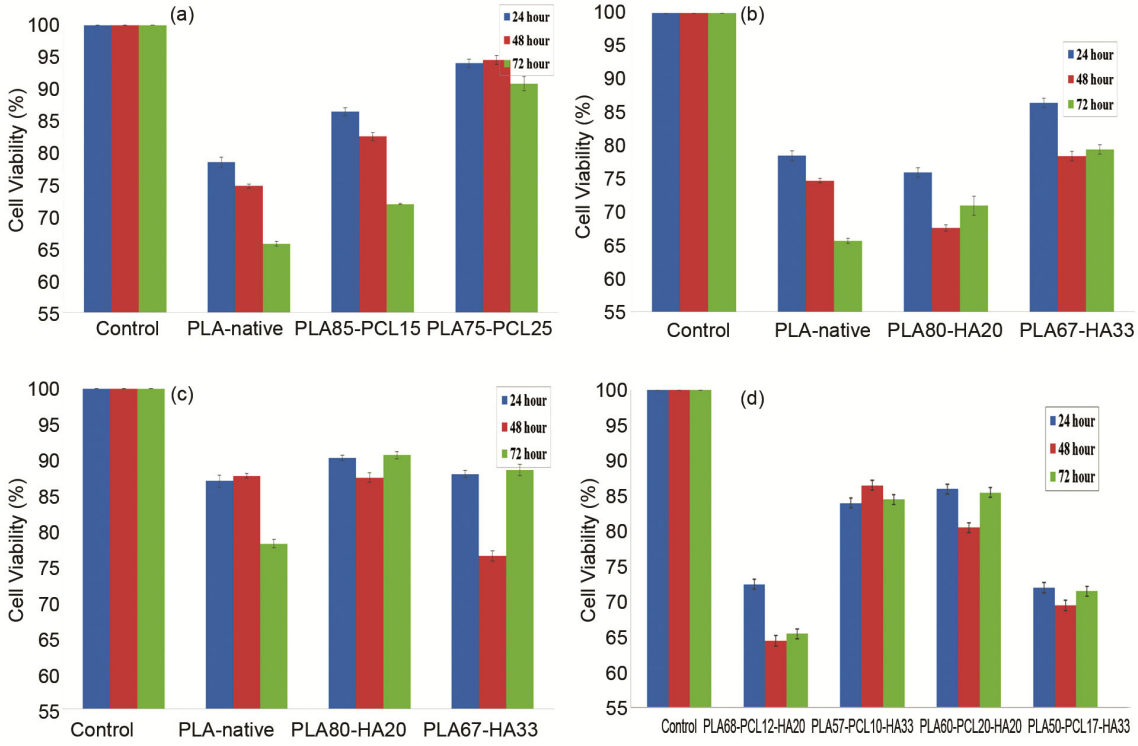

Fig. 13 — MTT–tetrazolium assay of L929 cultured in (a) PLA-PCL, (b) PLA-HA, (c) PCL-HA and (d) PLA-PCL-HA scaffolds for different times. Formosan absorbance is expressed as a function of scaffolds. (Error bars represent standard deviation).

percentages observed for pure PCL scaffold (PCL-native) were found to range between 78.2 and 87 % (Fig. 13c). The addition of hydroxyapatite showed similar effects on the cell viability. Increasing HA concentration increased the cell viability values to 78.5-86.5 % (Fig. 13b). PCL addition to solvent casted PCL-PLA scaffolds prepared in this work modified the polymer matrix consolidation/phase structure and dissolution behavior at pH = 7.4 improving the cell viabilities (Fig. 13a). The PLA68-PCL12-HA20 and PLA50-PCL17-HA33 composite scaffolds had the smallest crystallite sizes (5 and 7 nm, respectively) as seen in Fig. 9d which may indicate higher dissolution rates. This may be the reason for the lower cell viabilities observed for these two scaffolds (Fig. 13d). The composition of the composite scaffold structure has a determining role on the MTT cell viabilities.

4 Conclusion

PLA/PCL/HA 3D scaffolds with porosities 83-92% range were prepared by solvent-casting/salt-leaching method. HA addition to both PCL and PLA reduced the water absorption and porosity. Mechanical test results indicated an increase in strength of polymer matrix with HA additive. TGA analysis showed HA addition increased the degradation peak point. According to the Broido's model, degradation activation energy decreased with HA addition. According to the structural analysis with XRD before and after in vitro hydrolytic degradation, HA affected polimeric matrix consolidation and phase structure. The hydrolytic degradation study showed that degradation primarily occurs in the amorphous surface layer through diffusion. HA addition to PLA increased the diffusion coefficient whereas its addition to PCL decreased. Most of the cell viability of scaffolds increased with both PCL and HA.

Acknowledgements

The authors would like to thanks to Dr. Ahmet Yemenicioğlu for mechanical tests, Dr. Menemşe Gümüşderelioğlu from Hacettepe University Ankara Turkey for kindly supplying L929 cell lines, Izmir Institute of Technology Biothecnology and Bio-engineering Application and Research Center for MTT test especially Özgür Okur.

Conflict of Interest

The authors have no conflict of interests relating to the contents of the study presented in this manuscript. The authors have no conflict of interests related to financial or non-financial interests. All authors have participated in the WORK carried out in this paper.

References

1 Brahatheeswaran D, Yasuhiko Y, Toru M & Sakthi K D, *Int J Polym Sci*, 2011 (1687-9422).
2 Langer R, Fabrication of Biodegradable Polymer Foams for Cell Transplantation and Tissue Engineering, in: Morgan J R, Yarmush M L (Eds.), *Tissue Engineering Methods and Protocols* (Humana Press, Totowa, NJ), 1999, pp. 47.
3 Xiang Z, Liao R, Kelly M S & Spector M, *Tissue Eng*, 12(9) (2006) 2467.
4 Liang D, Hsiao B S & Chu B, *Adv Drug Deliv Rev*, 59(14) (2007) 1392.
5 Thomson R C, Wake M C, Yaszemski M J & Mikos A G, *Adv Polym Sci*, 122 (1995) 218.
6 Subia B, Kundu J, S C, *Biomaterial Scaffold Fabrication Techniques for Potential Tissue Engineering Applications* (In Tech, Rijeka), 2010.
7 Li X, Zhang S, Zhang X, Xie S, Zhao G & Zhang L, *Mater Design*, 114 (2017) 149.
8 Ulery B D, Nair L S & Laurencin C T, *J Polym Sci B Polym Phys*, 49(12) (2011) 832.
9 Rodenas-Rochina J, Vidaurre A, CastillaCortázar I & Lebourg M, *Polym Degrad Stab*, **119**(2015) 121.
10 Brekke J H & Toth J M, *J Biomed Mater Res*, 43(4) (1998) 380.
11 Dee K C & Bizios R, *Biotechnol Bioeng*, 50(4) (1996) 438.
12 Agapakis C M, *ACS Synth Biol*, 3(3) (2014) 121.
13 Fuchs J R, Nasseri B A & Vacanti J P, *Ann Thorac Surg*, 72(2) (2001) 577.
14 Tripathi G & Basu B, *Ceram Int*, 38(1) (2012) 341.
15 Hutmacher D W, *Biomaterials*, 21(24) (2000) 2529.
16 Elsawy M A, Kim K H, Park J W & Deep A, *Renew Sustain Energy Rev*, 79 (2017) 1346.
17 Tsuji H & Ikada Y, *Polym Degrad Stab*, 67(1) (2000) 179.
18 Paul M A, Delcourt C, Alexandre M, Degée P, Monteverde F & Dubois P, *Polym Degrad Stab*, 87(3) (2005) 535.
19 Lyu S & Untereker D, *Int J Mol Sci*, 10(9) (2009) 4033.
20 EyalA M &Canari R, *Ind Eng Chem*, 34(5) (1995) 1789-1798.
21 Kothapalli C R, Shaw M T & Wei M, *Acta Biomater*, 1(6) (2005) 653.
22 Zhu L & Bratlie K M, *Biochem Eng J*, 132 (2018) 38.
23 Chieng B, Ibrahim N &Yunus W, Hussein M, *Polymers*, 6(1) (2014) 93.
24 Choksia N & Desai H, *Int J Appl Chem*, 13(2) (2017) 377.
25 Elzein T, Nasser-Eddine M, Delaite C, Bistac S & Dumas P, *J Colloid Interface Sci*, 273(2) (2004) 381.
26 Gautam S, Dinda A K & Mishra N C, *Mater Sci Eng C*, 33(3) (2013) 1228.
27 Alp B &Cesur S, *J Appl Polym Sci*, 130(2) (2013) 1259.
28 Ślósarczyk Z, Paszkiewicz Z & Paluszkiewicz C, *J Mol Struct*, 744-747 (2005) 657.
29 Broido A, *J Polym Sci*, 7 (1969) 1761.
30 Balköse D, Egbuchunam T O & Okieimen F E, *J Therm Anal Calorim*, 101(2) (2010) 795.
31 Li J, Zheng W, Li L, Zheng Y & Lou X, *Thermochim Acta*, 493(1) (2009) 90.
32 Wang Y, Liu L &Guo S, *Polym Degrad Stab*, 95(2) (2010) 207.
33 Crank J, *The Mathematics of Diffusion* (Clarendon Press, Oxford), 2nd Edn, ISBN: 0198533446, 1975, p. 539.
34 International Organization for Standardization, *ISO 10993-5: 2009, Biological Evaluation of Medical Devices – Part 5: Tests for in vitro Cytotoxicity* (ISO, Geneva), 2009.